Alternating Layer and Island Growth of Pb on Si by Spontaneous Quantum Phase Separation

Hawoong Hong,[1] C.-M. Wei,[2,3] M. Y. Chou,[3] Z. Wu,[1,4] L. Basile,[1,5] H. Chen,[6] M. Holt,[1,5] and T.-C. Chiang[1,5]

[1]*Frederick Seitz Materials Research Laboratory, University of Illinois at Urbana-Champaign, 104 S. Goodwin Avenue, Urbana, Illinois 61801-2902*

[2]*Institute of Physics, Academia Sinica, Nankang, Taipei, Taiwan 11529, Republic of China*

[3]*School of Physics, Georgia Institute of Technology, Atlanta, Georgia 30332-0430*

[4]*Department of Materials Science and Engineering, University of Illinois at Urbana-Champaign, 1304 W. Green Street, Urbana, Illinois 61801-2980*

[5]*Department of Physics, University of Illinois at Urbana-Champaign, 1110 W. Green Street, Urbana, Illinois 61801-3080*

[6]*Department of Physics and Materials Science, City University of Hong Kong, 83 Tat Chee Avenue, Kowloon, Hong Kong, SAR, People's Republic of China*

(Received 2 August 2002; published 20 February 2003)

Real-time *in situ* x-ray studies of continuous Pb deposition on Si(111)-(7 × 7) at 180 K reveal an unusual growth behavior. A wetting layer forms first to cover the entire surface. Then islands of a fairly uniform height of about five monolayers form on top of the wetting layer and grow to fill the surface. The growth then switches to a layer-by-layer mode upon further deposition. This behavior of alternating layer and island growth can be attributed to spontaneous quantum phase separation based on a first-principles calculation of the system energy.

DOI: 10.1103/PhysRevLett.90.076104 PACS numbers: 68.55.Jk, 61.10.Kw

Thin film growth usually falls into one of three broad categories: Frank–van der Merwe (layer by layer), Volmer-Weber (island formation), and Stranski-Krastanov (layer growth followed by island formation) [1]. Each system adopts a unique growth mode depending on the relative magnitudes of the surface and interface energies. While this scheme of classification is well understood and works for the vast majority of systems investigated so far, the growth of Pb on Si(111)-(7 × 7) represents an interesting exception. Our real-time, *in situ* x-ray study shows an unusual growth behavior at 180 K. The initial growth is a flat wetting layer, followed by the formation of islands of a fairly uniform height of 5 ± 1 monolayers (ML). These islands then grow to fill the surface, and layer-by-layer growth takes over on further deposition. This observation of magic or critical thicknesses for growth mode switching suggests that quantum size effects play an important role [2]. Indeed, previous scanning tunneling microscopy and electron diffraction studies of the film morphology of Pb/Si have revealed preferred island heights under certain experimental conditions, and quantum size effects have been postulated to be the cause [3–5]. Similar observations have been reported for other substrates as well [6]. However, the observed magic island height in this case bears no obvious relation to any known characteristic lengths of the quantum electronic structure of the system, and no theories or models yet exist to explain the overall growth pattern. To solve this puzzle, we have performed first-principles model calculations of the system energy. The calculated energy as a function of film thickness reveals Friedel-type oscillations riding on an envelope function, resulting in two deep minima which can be identified as the wetting layer thickness and the magic island height. Coverages in between yield an unstable system that spontaneously phase separates into a combination of a wetting layer and the magic-height islands. This type of quantum phase separation is similar to that seen in classical systems with a miscibility gap which can evolve via spinodal decomposition, nucleation, and growth. An important concept demonstrated here is that the global energy landscape, rather than the local stability as emphasized in previous film studies [2,7], is key to understanding this type of film growth.

To determine the film morphology evolution *in situ* during deposition at a steady rate, we employed an undulator beam of 26.05 keV x rays from Sector 33, UNICAT (University-National Laboratory-Industry Collaborative Access Team), Advanced Photon Source, Argonne National Laboratory, to measure the reflectivity and the Pb(10L) truncation rod. A charge-coupled device (CCD) was used to capture the Pb rod over a wide range of momentum transfer. This was made possible by a small mosaic spread within the Pb film resulting in a broadened rod that intersected over a range of L with the rather large, nearly tangent Ewald sphere. Pb was deposited from an effusion cell at a constant rate, monitored by a quartz thickness monitor, onto a freshly prepared Si(111)-(7 × 7) substrate. The temperature of the sample, measured by a thermocouple welded to the metal support of the substrate, was set at 180 K during growth.

Typical CCD images (Fig. 1) taken at various times of deposition at a constant deposition rate of 0.0044 ML per second show the gradual development of multilayer interference fringes along the Pb(10L) rod. At high coverages Pb Bragg peaks at (101) and (102) appear as indicated in the figure, which are surrounded by satellite peaks. These interference fringes yield information about

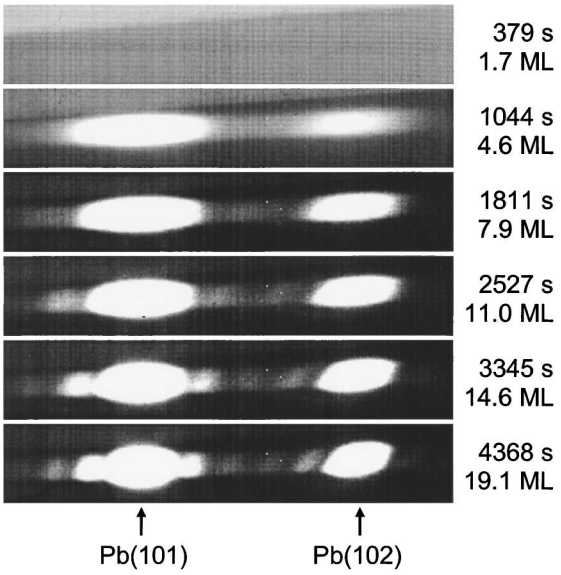

FIG. 1. A set of x-ray diffraction images captured by a CCD during Pb growth on Si(111) at times (and corresponding coverages) indicated. Each image shows a section of the Pb(10L) rod, and the Pb(101) and Pb(102) Bragg peaks are indicated.

layer thickness and island height. Our analysis employs a hexagonal surface coordinate system (h), which is related to the usual cubic lattice (c) by

$$(001)_h = \tfrac{1}{3}(111)_c, \qquad (010)_h = \tfrac{1}{3}(22\bar{4})_c,$$
$$(100)_h = \tfrac{1}{3}(4\bar{2}2)_c.$$

The growth consists of both (111) and $(\bar{1}\bar{1}\bar{1})$ domains, and the peak at (101) is actually $(\bar{1}01)$ for the $(\bar{1}\bar{1}\bar{1})$ growth. The (102) peak appears weaker due to the curvature of the Ewald sphere and its reduced overlap with the rod. This varying degree of overlapping is taken into account in our analysis of the results.

Detailed rod profiles are extracted from the detector images, and the overall growth behavior is illustrated by a sequence of rod profiles in Fig. 2(a), taken at various times from $t = 0$ to 4350 s for a total coverage of $N = 19$ ML. These rod profiles are displayed on the same intensity scale but offset vertically from trace to trace for display clarity. Selected rods at the initial stages of film growth are displayed in Fig. 2(c) with an amplified vertical scale. The results show a featureless background with no Pb diffraction until t reaches between 327 and 379 s (~ 1.5 ML total coverage). At that time, the Pb peaks suddenly emerge. The Si(10) surface diffraction spot, measured simultaneously but not presented here, shows a rapid increase in intensity for the first ~ 1.1 ML of deposition and a slight decline afterwards. This can be attributed to the formation of a Pb wetting layer that is somewhat compressed and commensurate with the Si substrate [8]. Pb has a large scattering cross section, and

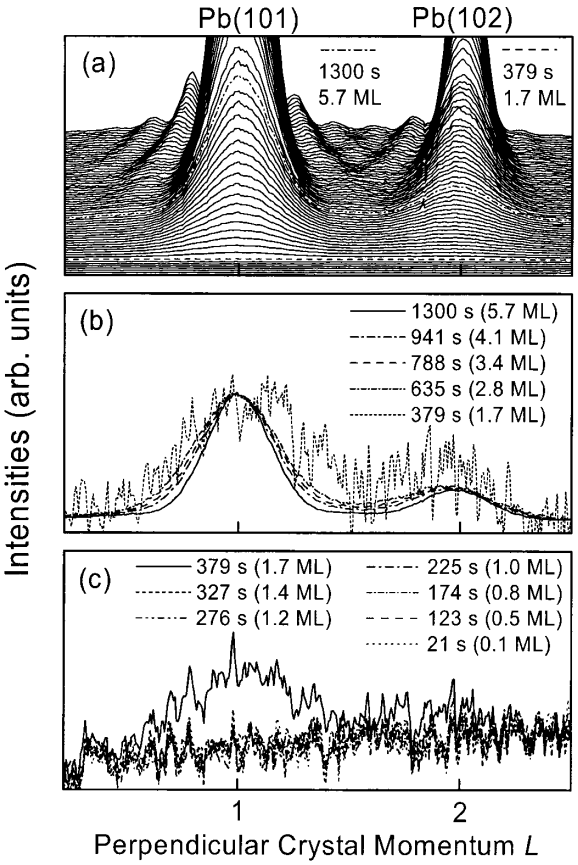

FIG. 2. (a) A set of scans of the Pb(10L) rod taken successively while Pb is being deposited on Si(111). The traces are normalized and are offset vertically for clarity. The time interval between successive traces is 51 s, and the deposition rate is 0.0044 ML/s. (b) Some of the scans taken after the completion of the wetting layer are shown renormalized to the same peak height to illustrate the approximately constant line shape during the lateral growth phase of the islands. A background function, represented by the scan at $t = 327$ s, is subtracted. (c) Some of the initial traces are shown to illustrate the lack of Pb diffraction during the formation of the wetting layer and the sudden onset of the Pb features after the completion of the wetting layer.

decorating the Si(111) surface by Pb can lead to a strongly enhanced intensity at the Si surface peak positions, but little intensity at the Pb positions. Additional coverage of Pb beyond the completion of the wetting layer results in a two-dimensional gas of Pb adatoms which contribute to neither the Pb nor the Si diffraction. The pressure of this gas builds up and at ~ 1.5 ML total coverage islands begin to form [3].

The Pb islands, once formed, remain fairly constant in height for the next several ML of Pb deposition. As seen in Fig. 2(b), the rod profiles, background subtracted and normalized to the same peak height, remain nearly the same for coverages up to ~ 6 ML. A detailed analysis of the (101) and (102) peak widths and of the rod profiles by fitting shows that the films consist of Pb islands with a

fairly uniform height of 5 ± 1 ML above the wetting layer. Thus, increasing Pb deposition within this range results in mainly lateral growth of the islands. The overall intensity of the rod increases in proportion to the total area covered by the islands, and the signal to noise ratio improves as seen in the figure.

The full set of rod profiles in Fig. 2(a) indicates that, after the surface becomes fully covered by the islands, the film growth switches to a layer-by-layer mode. This is evidenced by the smooth evolution of well-developed satellite peaks that represent multilayer interference fringes. Fringe counting allows a straightforward determination of the film thickness. The addition of each satellite peak between (101) and (102) corresponds to an increment of the film thickness by 3 ML. Thus, the top trace, with four satellite peaks in between (101) and (102), correspond to $(4 + 2) \times 3 = 18$ ML above the wetting layer, or a total coverage of $N = 19$ ML including the wetting layer.

The observation of two critical thicknesses corresponding to the wetting layer and the magic-height islands strongly suggests quantum size effects as the underlying cause. However, the magic island height does not correspond to any known characteristic lengths associated with the quantum electronic structure. To gain some insight, we have carried out first-principles total-energy calculations for a model system using the Vienna *ab initio* simulation package based on density-functional theory within the local density approximation [9]. Since Pb and Si are not lattice matched, a full calculation with two incommensurate in-plane lattice constants are not feasible with a finite unit cell. Instead, the calculation is carried out with the Si compressed by 8.8% to conform to the Pb lattice constant. A supercell geometry is employed, and each supercell consists of a vacuum region with a thickness equivalent to 10 ML of Pb, a Pb film, and a slab of five bilayers of Si as the substrate with its back side terminated by H. A similar calculation is also carried out for freestanding Pb films without the Si substrate [10] for comparison in order to investigate the possible Pb/Si interface effects on the film properties. Despite the artificial compression of the Si substrate, this model retains the essential physics pertaining to quantum confinement [11]. Each Pb monolayer added to the film results in discrete changes in the electronic structure, and the system energy shows substantial quantum variations at small film thicknesses. For both the freestanding and supported films, the total energy per surface atom depends linearly on N at large N. This linear dependence and the substrate contribution are subtracted away to yield a relative surface energy $E_S(N)$ [12], which provides a measure of the relative stability of different film thicknesses. The energy reference is chosen such that $E_S(0) = 0$.

Figure 3(a) shows the calculated $E_S(N)$ for the freestanding films. It exhibits damped Friedel-type oscillations with a period of oscillation of $\lambda = 1.8$ ML, which is

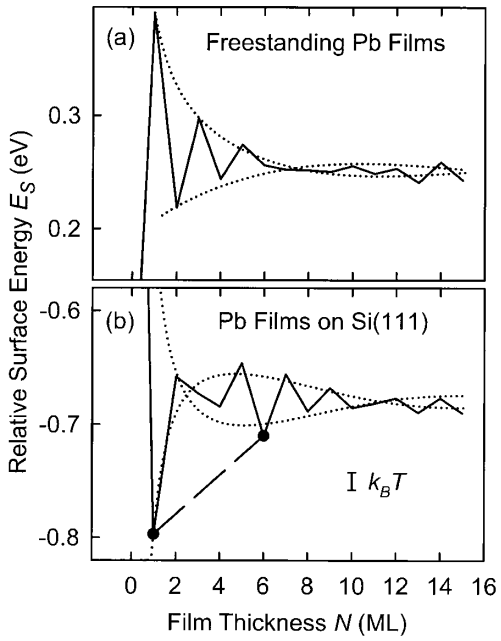

FIG. 3. (a) Calculated relative surface energy per surface atom for freestanding Pb films as a function of layer thickness N. (b) The same for Pb films on Si. In both cases, $E_S(0) = 0$. The dotted curves represent envelope functions for the quantum oscillations.

one-half of the Fermi wavelength in Pb [13]. This period is close, but not quite equal, to an integer value (2 ML). The small difference yields a beating pattern with an envelope function of a period (internode distance) of $\lambda/(2 - \lambda) = 9$ ML. This energy curve can be described approximately by a simple asymptotic form [2], and the envelope functions derived from such a model fit are shown in the figure as dotted curves. A node in the envelope function is evident at $N \sim 7$, near which the 1.8 ML period oscillations are suppressed. Figure 3(b) shows the results for Pb films on Si. Oscillations at the same 1.8 ML period are also present, as this is a universal feature of quantum confinement. The change in boundary condition, however, introduces an extra phase shift of about $0.4 \times \pi$. This causes the envelope function to shift, with the first antinode now at $N = 6$. The result is a deep minimum at $N = 6$, in addition to the absolute minimum at $N = 1$.

The absolute minimum at $N = 1$ would favor the formation of a wetting layer at this thickness at the initial stages of deposition. For coverages between 1 and 6 ML, the system would phase separate by spontaneous decomposition into a linear combination of $N = 1$ and 6. The dashed line in Fig. 3(b) shows the energy of the phase-separated system, which is clearly lower than the original curve. This predicted phase separation is in excellent agreement with the observation. Experimentally, the system forms a wetting layer of thickness $N = 1$ followed by island formation with a height of ~5 ML. The total

thickness over the areas covered by the islands, including the initial wetting layer, is thus $N = 6$. This excellent agreement can be partly attributed to the simplicity of the free-electron-like structure of Pb. The shape of the energy curve is essentially governed by a single parameter—the phase shift at the Pb-Si boundary. This is well reproduced by the calculation despite the simplification in the modeling. An interesting point about the graphs in Fig. 3 is that E_S for a monolayer film ($N = 1$) is positive for a freestanding film, but negative for a supported film. The reason for a positive E_S in the former case is that it costs energy to create a surface from bulk Pb. If a freestanding monolayer film is bonded to a Si substrate, the total energy is substantially lowered due to chemical bonding at the interface, thus leading to a large negative E_S.

Growth kinetics could potentially hinder the phase separation and trap the system in other nearby minima, such as the one at $N = 4$. However, the thermal energy k_BT at the growth temperature, indicated in Fig. 3(b) by a vertical bar, is comparable to the other shallower minima, and trapping appears to be a relatively minor effect. This is consistent with the observation that the islands form as soon as the wetting layer is complete, which further implies rapid and facile diffusion of adatoms on the surface and over the island edges. Thus, the system is in a quasiequilibrium condition at the growth temperature. At higher coverages beyond the phase-separation region, the quantum variations in surface energy diminish rapidly, and the system maintains a nominal layer-by-layer growth in order to minimize step and kink energies [14].

Studies of stability and growth of nanostructures and films have traditionally focused on the second derivative of the system energy [2,7,15]. This yields a prediction for local stability, namely, whether the film would bifurcate ($N \rightarrow N \pm 1$). In the present case, such an analysis would yield a prediction for stability with a $\sim$2 ML period of oscillation [2], and one might be tempted to conclude that films with either even or odd numbers of layers are to be observed during growth. Our work shows that it is important to consider the global energy landscape as well as the growth kinetics for a correct and complete prediction of the growth behavior.

This work is supported by the U.S. Department of Energy (Grants No. DEFG02-91ER45439 and No. DEFG02-97ER45632), the R.O.C. National Science Council (Grant No. 90-2112-M-001-062), the U.S. National Science Foundation (Grants No. DMR-02-03003 and No. SBE-01-23532), and the Petroleum Research Fund administered by the American Chemical Society. The UNICAT facility at the Advanced Photon Source (APS) is supported by the University of Illinois Frederick Seitz Materials Research Laboratory (U.S. Department of Energy and the State of Illinois-IBHE-HECA), the Oak Ridge National Laboratory (U.S. Department of Energy under contract with Lockheed Martin Energy Research), the National Institute of Standards and Technology (U.S. Department of Commerce), and UOP LLC. The APS is supported by the U.S. Department of Energy (Grant No. W-31-109-ENG-38).

[1] A. Zangwill, *Physics at Surfaces* (Cambridge University Press, New York, 1988).
[2] Z. Zhang, Q. Niu, and C. K. Shih, Phys. Rev. Lett. **80**, 5381 (1998).
[3] L. Gavioli, K. R. Kimberlin, M. C. Tringides, J. F. Wendelken, and Z. Zhang, Phys. Rev. Lett. **82**, 129 (1999); K. Budde, E. Abram, V. Yeh, and M. C. Tringides, Phys. Rev. B **61**, R10 602 (2000); M. Hupalo, S. Kremmer, V. Yeh, L. Berbil-Bautista, E. Abram, and M. C. Tringides, Surf. Sci. **493**, 526 (2001).
[4] W. B. Su, S. H. Chang, W. B. Jian, C. S. Chang, L. J. Chen, and T. T. Tsong, Phys. Rev. Lett. **86**, 5116 (2001).
[5] I. B. Altfeder, K. A. Matveev, and D. M. Chen, Phys. Rev. Lett. **78**, 2815 (1997).
[6] R. Otero, A. L. V. de Parga, and R. Miranda, Phys. Rev. B **66**, 115401 (2002).
[7] D.-A. Luh, T. Miller, J. J. Paggel, M. Y. Chou, and T.-C. Chiang, Science **292**, 1131 (2001).
[8] H. H. Weitering, D. R. Heslinga, and T. Hibma, Phys. Rev. B **45**, 5991 (1992). Our measured wetting layer coverage of 1.1 ML in terms of the Pb lattice is equivalent to 4/3 ML in terms of the Si lattice.
[9] G. Kresse and J. Furthermuller, Phys. Rev. B **54**, 11 169 (1996), and references therein.
[10] C. M. Wei and M. Y. Chou, Phys. Rev. B **66**, 233408 (2002). A similar calculation for freestanding films can be found in G. Materzanini, P. Saalfrank, and P. J. D. Lindan, Phys. Rev. B **63**, 235405 (2001).
[11] T.-C. Chiang, Surf. Sci. Rep. **39**, 181 (2000).
[12] J. C. Boettger, J. R. Smith, U. Birkenheuer, N. Rösch, S. B. Trickey, J. R. Sabin, and S. P. Apell, J. Phys. Condens. Matter **10**, 893 (1998).
[13] The Fermi wave vector of Pb along [111] is 1.59 Å^{-1} in the extended zone. Here we use the reduced-zone value of 0.61 Å^{-1} as measured from the zone center. See A. P. Cracknell, in *Metals: Phonon and Electronic States, Fermi Surfaces*, edited by K.-H. Hellwege and J. C. Olsen, Landolt-Börnstein, New Series, Vol. III, Pt. 13c (Springer-Verlag, Berlin, 1984), p. 275.
[14] The system may exhibit a degree of preferred bilayer growth around $N = 6$, but the evidence is inconclusive in the present data.
[15] W. D. Knight, K. Clemenger, W. A. de Heer, W. A. Saunders, M. Y. Chou, and M. L. Cohen, Phys. Rev. Lett. **52**, 2141 (1984).